Med Biol Eng Comput (2015) 53:393–403
DOI 10.1007/s11517-014-1241-z

ORIGINAL ARTICLE

# Hemodialysis vascular access stenosis detection using auditory spectro-temporal features of phonoangiography

**Po-Hsun Sung · Chung-Dann Kan · Wei-Ling Chen · Ling-Sheng Jang · Jhing-Fa Wang**

Received: 10 July 2014 / Accepted: 28 December 2014 / Published online: 15 February 2015


**Abstract** For end-stage renal disease patients undergoing hemodialysis, thrombosis caused by stenosis hinders the long-term use of vascular access. However, traditional spectral bruit analysis techniques for detecting the severity of vascular access stenosis are not robust. Accordingly, the present study proposes an automated method for mimicking a trained practitioner in performing the auscultation process. In the proposed approach, the bruit obtained using a standard phonoangiographic method is transformed into the time–frequency domain, and two spectro-temporal features, namely the auditory spectrum flux and the auditory spectral centroid, are then extracted. The distributions of the two features are analyzed using a multivariate Gaussian distribution (MGD) model. Finally, the distribution parameters of the MGD model are used to detect the presence (or otherwise) of vascular access stenosis. The validity of the proposed approach is investigated using the phonoangiography signals obtained from 16 hemodialysis patients with straight arteriovenous grafts over the upper arm region. The results show that the MGD covariance matrix coefficient of the auditory spectral centroid feature yields an accuracy of 83.87 % in detecting significant vascular access stenosis. Thus, the proposed method has significant potential for the applications of vascular access stenosis detection.

**Keywords** Hemodialysis · Vascular access stenosis · Auditory spectrogram · Auditory spectrum flux · Auditory spectral centroid

P.-H. Sung (✉) · L.-S. Jang (✉) · J.-F. Wang
Department of Electrical Engineering, National Cheng Kung University, No. 1, University Road, Tainan City 701, Taiwan, ROC
e-mail: phsung@gmail.com

L.-S. Jang
e-mail: lsjang@ee.ncku.edu.tw

C.-D. Kan
Department of Surgery, National Cheng Kung University Hospital, No. 138, Sheng Li Road, Tainan City 704, Taiwan, ROC

W.-L. Chen
Department of Biomedical Engineering, National Cheng Kung University, No. 1, University Road, Tainan City 701, Taiwan, ROC

## 1 Introduction

Hemodialysis is an essential treatment for removing waste products and excess fluid from the blood of end-stage renal disease (ESRD) patients [37]. The permanent vascular access connects an artery and a vein to provide sufficient blood flow to access dialysis. In performing hemodialysis, permanent vascular access is generally obtained using arteriovenous (AV) fistulas, AV grafts or venous catheters [16]. However, following prolonged usage, irreversible thrombosis caused by stenosis hinders the use of vascular access [12]. Accordingly, reliable surveillance methods for detecting vascular access stenosis at an early stage of development are essential in facilitating remedial treatment such as percutaneous transluminal angioplasty (PTA) [2]. PTA is an invasive procedure to dilate the lumen of the stenotic site in the vascular access [34].

The literature contains various proposals for detecting hemodynamically significant vascular access stenosis [3, 13, 27, 29, 40]. For example, the noninvasive imaging techniques, namely magnetic resonance (MR) angiography, are currently used for detecting stenosis in the cardiovascular system [3]. However, while such methods provide an accurate indication of the degree of vascular access stenosis, they require the use of expensive apparatus and involve

certain surgical risks in using catheterization and contrast [13]. Accordingly, various authors have proposed noninvasive methods for detecting the lumen narrowing in the vascular access region by means of ultrasound imaging techniques [27, 29]. Currently, ultrasonic detection method has become a standard procedure to evaluate the vascular stenosis in the hospital [40]. However, the methods proposed in [3, 13, 27, 29, 40] are highly skill dependent and are impractical for initial screening in hemodialysis centers.

Phonoangiography is a noninvasive and inexpensive procedure for evaluating the sound pattern of bruit produced by the local blood flow through the vascular system [24, 28]. When blood flows through a constricted blood vessel, the resulting flow jet induces a turbulent flow and a pressure fluctuation in the blood vessel wall [31]. The resulting acoustic noise emitted from the vessel is defined as a murmur or bruit. Knox et al. [21] used a spectral bruit analysis (SBA) method to evaluate the severity of the carotid artery stenosis. Lees [23] founded that the peak systolic portion of the bruit processed by fast Fourier transform (FFT) is directly related to the residual lumen diameter of the stenotic internal carotid artery. Mansy et al. [25] evaluated the vascular patency of hemodialysis access by measuring the spectral change of the SBA. However, the disadvantage of SBA is their narrow sharp peaks induced from FFT calculation, which is hard to implement the spectral peak analysis in programming. Chen et al. [8, 9] proposed a method based on the Burg autoregressive (AR) model combined with fractional-order chaos system and fuzzy petri nets (FPNs) to evaluate the relationship between the power spectral density (PSD) and the vascular access degree of stenosis (DOS). Notably, the methods proposed in [8, 9, 21, 23, 25] are all based on a spectral analysis of the phonoangiography signal. In practice, phonoangiography is recorded with the mixture of ambient environment noise and friction noise generated by the movement of sensor head. The unwanted noises sometimes have similar spectral information as bruit caused by the turbulent blood flow in the narrow blood vessel. Only using spectral information is hard to directly distinguish the dynamic characteristics of bruit directly from noisy phonoangiography. However, the clinicians can recognize the stenosis sound pattern in noisy environments. The auditory perception mechanism is based on the basilar membrane mechanical response induced by sound and more sensitive to the transient response than steady-state signal. Thus, intuitively, the auditory perception models are considered when performing bruit analysis approach. In our proposal, the auditory spectrogram and auditory spectro-temporal features are used to overcome the limits in traditional time–frequency representation (TFR) methods.

Auscultation is a noninvasive procedure to initially evaluate the vascular access stenotic signs in hemodialysis patients. However, the outcome of auscultation is both subjective and skill dependent. Consequently, great interest exists in visualizing the time–frequency pattern of the auscultation signal so as to obtain a more objective and reliable prediction of the stenosis degree. Time–frequency representation (TFR) methods are widely used to analyze biomedical signals such as phonocardiograms [6]. Among the various TFR methods, the short-time Fourier transform (STFT) method uses a simple FFT operation to analyze the time signal. However, the fixed resolution of STFT is a compromise for the analysis of non-stationary signals [7]. In the wavelet transform (WT) method, the WT overcomes the fixed resolution limitation of STFT to get enormous spectral-temporal information and is suitable for analyzing the non-stationary biomedical signal [14]. However, the performance of WT is critically dependent on the choice of basis kernel function, e.g., Morlet, Daubechies [10].

In a previous study, Sung et al. [32] presented a computer-assisted auscultation approach for detecting abnormal heart sounds due to congenital heart disease. The present study proposes a similar system integrated with auscultation technique to evaluate vascular access stenosis. Figure 1 presents a functional block diagram of the proposed method. As shown, the phonoangiography signal is obtained by the ESRD patient. The signal is then transformed into an auditory spectrogram in the time–frequency domain using a process mimicking that of the human ear. Two spectro-temporal features of the spectrogram, namely the auditory spectrum flux (ASF) and the auditory spectral centroid (ASC), are then extracted and processed using a multivariate Gaussian distribution (MGD) model. Finally, the presence of stenosis is detected by examining the distributions of the two features in the MGD model.

## 2 Materials and methods

### 2.1 Subjects and experimental procedure

Sixteen hemodialysis patients (four male and 12 female; mean age 60.5 ± 10.0 years) were invited to participate in the study. All of the participants had straight type AV grafts over the upper arm region. The institutional review board (IRB) of National Cheng Kung University Hospital approved both the data collection process for the 16 patients and the follow-up tracking program, under the IRB protocol No. ER-99-186. For each patient, phonoangiography signals were recorded continuously over a minimum period of 20 s to ensure getting ten pulse cycles segmentation for further analysis. The recording process will be repeated until the extracted phonoangiography signals are stable without surrounding noise interference. Moreover, the bruits were acquired at both the arterial anastomosis site (A-site) and the venous anastomosis site (V-site) before and

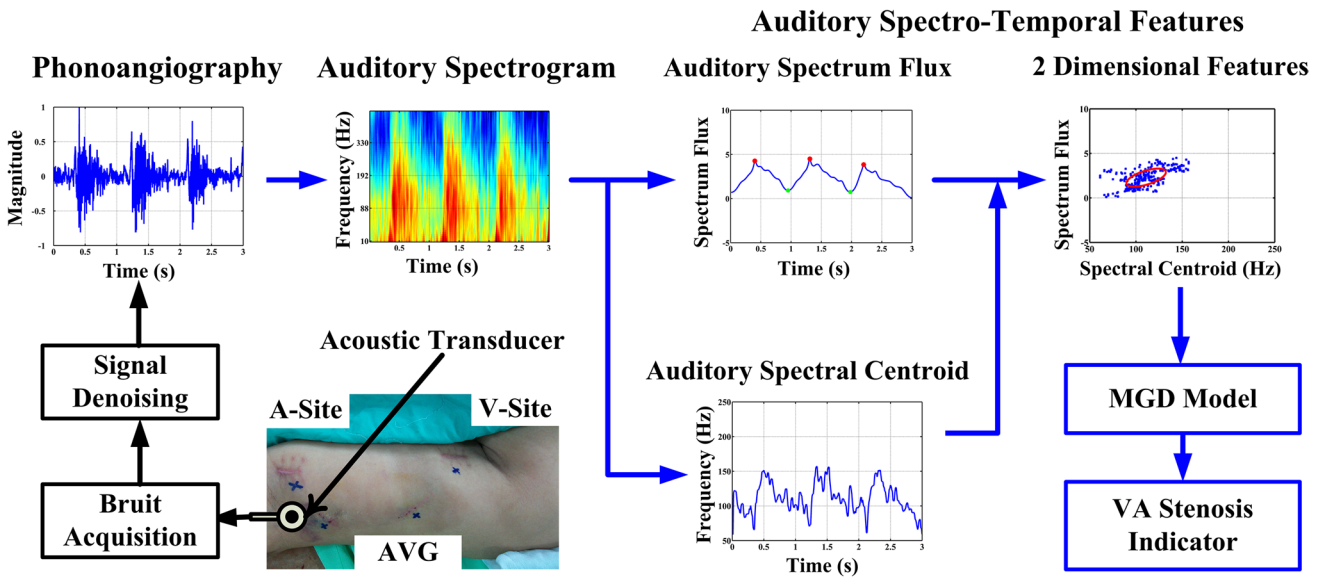


**Fig. 1** Functional block diagram of proposed auditory auscultation system for hemodialysis vascular stenosis detection

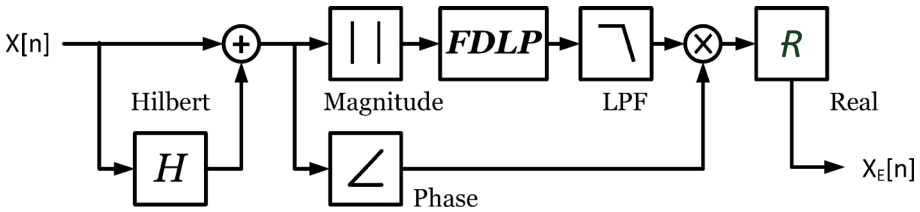


**Fig. 2** Procedure of signal denoising method based on demodulation technique

after undergoing PTA treatment. The bruits were recorded using an electronic stethoscope (3 M LITTMANN® 4100 series) with a sampling rate of 4,000 Hz and a resolution of 16 bits. The phonoangiography was then converted into an auditory spectrogram, and the spectro-temporal features extracted and processed, using a self-written program implemented in Matlab®.

## 2.2 Signal denoising

The sound signals acquired by an acoustic transducer generally contain unexpected interference as a result of environmental noise and motion artifacts. Therefore, the denoising operation to improve robust signal acquisition is required. Lee and Zhang [22] proposed a method for reducing the effects of motion artifacts in photoplethysmographic recordings using a wavelet threshold approach. However, the optimal value of the threshold was set in accordance with a trial-and-error approach and was not suitable for all of the considered subjects. As described in Sect. 1, the blood flow through a stenotic region has the form of a pulsatile flow. Thus, it is reasonable to assume that the phonoangiography signal is effectively a modulation signal. Accordingly, in the present study, the phonoangiography signals are denoised by removing the high-frequency noise interference components using the demodulation technique, as shown in Fig. 2.

In developing the demodulation scheme, it is assumed that a discrete input signal $x[n]$ can be expressed as the sum of the clean signal $s[n]$ and the additive noise $e[n]$, i.e.,

$$x[n] = s[n] + e[n]. \tag{1}$$

where the noise $e[n]$ may result from a combination of ambient noisy sound, instrument noise, frictional noise of sensor head and physiological acoustic noise from body.

The input signal $x[n]$ can then be normalized in the preprocessing stage as follows:

$$x_N[n] = x[n]/\max|x[n]|, \tag{2}$$

where $x_N[n]$ denoted the normalized bruits signal.

In mathematics, an analytic signal can be represented as the sum of a real part and an imaginary part [18]. It can also be specified as exponential form or joint both compositions of amplitude modulation (AM) and frequency modulation (FM), as follows:

$$\begin{aligned} x_a[n] &= x_N[n] + j\mathrm{H}\{x_N[n]\} \\ &= \mathrm{AM}[n] \cdot \exp\{j\phi_m[n]\}, \end{aligned} \tag{3}$$

where H{·} is the Hilbert transform; AM[$n$] = $\|x_a[n]\|$ denotes an instantaneous amplitude or AM envelope; $\phi_m[n]$ is instantaneous phase of $x_a[n]$; note that the derivative of $\phi_m[n]$ is instantaneous frequency (IF).

Hilbert transform is one of the demodulation techniques to estimate the envelope of AM and the IF of the signal. However, the Hilbert envelope is sensitive to high-frequency modulation interference [11]. Thus, in the proposed system, the envelope of the phonoangiography signal is further estimated by means of autoregressive modeling technique, namely frequency domain linear prediction (FDLP) [35].

The $N$-dimensional real vector which represents a finite-duration discrete-time AM envelope AM[$n$] is processed by forward discrete cosine transform (DCT). The DCT property of AM[$n$] can be calculated by approximating the discrete Fourier transform (DFT) of the AM envelope. Then, the DCT of AM can be extracted as

$$\mathrm{AM}_{\mathrm{DCT}}[k] = a[k]|\mathrm{AM}_{\mathrm{DFT}}[k]| \cos\left(\theta[k] - \frac{\pi k}{2N}\right), \quad k = 0, 1, \ldots, N-1, \tag{4}$$

where the $|\mathrm{AM}_{\mathrm{DFT}}[k]|$ and $\theta[k]$ are the magnitude and phase of the zero-padded DFT sequence, respectively, and $N$ is the signal samples of the discrete enhanced phonoangiography signal.

Moreover, the linear predictions of the DCT components calculated by the autocorrelation method are taken as the output of the FDLP process [5]. The AM envelope calculated using the FDLP technique is then passed through a zero-phase low pass filter in order to remove the high-frequency modulation interference and obtain the enhanced AM envelope (as shown in the red solid lines in Fig. 3a, b). Finally, the enhanced AM envelope is multiplied by the original FM signal to reconstruct the enhanced phonoangiography signal, shown in Fig. 2.

### 2.3 Auditory time frequency representation

In the proposed auditory auscultation method, the bruits are transformed into the time–frequency plane using a cochlear wavelet transform (CWT) module, which mimics the auditory response of the human ear. The CWT module modified the gammachirp function presented by Irino [20] as complex-valued cochlear wavelet function to better characterize the level-dependent mechanical motion of the basilar membrane as follows:

$$\psi_{a,b}[t] = [t]^{\alpha-1} \exp\left\{-j2\pi\beta \cdot \mathrm{ERB}\left[f_{\mathrm{center}}\right] \cdot [t]\right\} \cdot \exp\left\{j2\pi f_{\mathrm{center}}[t] + j\gamma \ln[t] + \varphi\right\}, \tag{5}$$

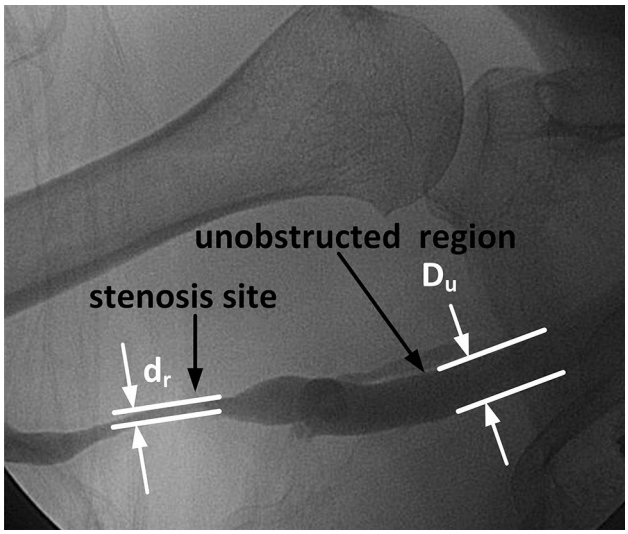


**Fig. 3** Angiogram of the stenosis site in hemodialysis patient with arteriovenous access

where $\alpha$ and $\beta$ are parameters describing the envelope of the gamma distribution, $\alpha = 4$, $\beta = 1.019$ are used in this paper; $f_{\mathrm{center}}$ is the critical center frequency; $\gamma$ is the chirp term; $\varphi$ is the initial phase; $t$ is $t = [b - n]/a_i$, $n$ is the analyzed sample index, $a_i$ is the scale factor of each frequency bin $i$; $b$ is the sample location variable, and the term $\mathrm{ERB}[f_{\mathrm{center}}]$ is the equivalent rectangular bandwidth which varies with the center frequency [19].

In implementing the CWT into mathematical software, the output of the CWT module is modeled as the convolution of the enhanced phonoangiography signal $x_E[n]$ with the $K$ analyzed wavelet functions, i.e.,

$$\mathbf{AS}[k, n] = \sum_{k=1}^{K} \frac{1}{\sqrt{a_i}} \psi_{a,b}[k, n] \times x_E[n], \tag{6}$$

where $\mathbf{AS}[k, n]$ is the complex-valued output of the discrete CWT, $k$ is the index of the analyzed wavelet function which can be regarded as frequency bin; $K$ is the total number of frequency bin, this paper adapts $K = 64$;

As described above, the magnitude of the CWT output, i.e., $\mathbf{AS}|[\mathrm{k}, \mathrm{n}]|$ gives the auditory spectrogram shown in Fig. 1 and represents the characteristics of the bruits in the time–frequency domain.

### 2.4 Auditory spectro-temporal features

In the system proposed in this study, the detection of vascular access stenosis is performed by means of two spectral-temporal features extracted from the auditory spectrogram, namely the ASF and the ASC.

#### 2.4.1 Auditory spectrum flux

The ASF feature provides an indication of the rate at which the magnitude of the auditory spectrum changes. The ASF feature is typically used to classify the types of audio signals and is defined as the average variation value of the auditory spectrum magnitude between two adjacent time frames [23]. In terms of stenosis detection, the peaks of time-varied ASF curve become sharp means that the severity of DOS increases. The spectrum flux of the auditory spectrogram is calculated by taking the ordinary Euclidean norm of the auditory spectrum magnitude difference with time, i.e.,

$$\mathrm{SF}[n] = \frac{1}{K}\sqrt{\sum_{k=1}^{K}[|\mathbf{AS}[k,n]| - |\mathbf{AS}[k,n-1]|]^2}. \tag{7}$$

#### 2.4.2 Auditory spectral centroid

In a practical auscultation procedure, pitch variation is taken as an important indicator of the severity of stenosis. The auditory pitch can be defined as the attribute of the auditory sensation in terms of the frequency components of the sound. Moreover, the spectral centroid provides a convenient approach for parameterizing the center of gravity of the magnitude auditory spectrum, which corresponds to the brightness of the sound [36]. Accordingly, in the present study, the ASC feature of the auditory spectrogram is used to model the auditory pitch of the phonoangiography signal. Mathematically, the ASC feature can be modeled as

$$f_{\mathrm{centroid}}[n] = \frac{\sum_{k=1}^{K}(|\mathbf{AS}[k,n]| \cdot f_{\mathrm{center}}[k])}{\sum_{k=1}^{K}|\mathbf{AS}[k,n]|}. \tag{8}$$

The spectral distribution of the bruits varies in accordance with the degree of narrowing of the stenosis region. Therefore, the severity of vascular access stenosis can be evaluated by monitoring the variation of the ASC feature. More specifically, a more intense and higher-pitched sound (i.e., a higher time-variation ASC curve) suggests the possible presence of stenosis, while little or no sound suggests a completely occluded condition.

#### 2.4.3 Multivariate Gaussian distribution

In the present study, the ASF and ASC features described above are redrawn as two-dimensional data distribution in ASC–ASF plane (i.e., $x$-, $y$-axis represents ASC and ASF, respectively) to describe the severity of the vascular access stenosis. As shown in Fig. 1, the distribution density of the two-dimensional data is described using a MGD model. The MGD function can be expressed as [33]

$$g(\mathbf{x}|\mu_i, \Sigma_i) = \frac{1}{(2\pi)^{D/2}|\Sigma_i|^{1/2}} \cdot \exp\left\{-\frac{1}{2}(\mathbf{x}-\mu_i)^{\mathrm{T}}\Sigma_i^{-1}(\mathbf{x}-\mu_i)\right\}, \tag{9}$$

where $\mathbf{x}$ represents the $D$-dimensional valued data, $D = 2$ for both ASC and ASF, $i$ is the mixture weights of the Gaussian density components, $\mu_i$ is the mean value of MGD and $\Sigma_i$ is the MGD covariance matrix.

The parameters of the MGD model can be estimated using the iterative expectation–maximization (EM) algorithm [39]. Furthermore, the mean values and covariance matrix coefficients of the MGD model can then be used to obtain a qualitative assessment of the presence of vascular access stenosis.

## 3 Results

In this study, 64 bruits distributed over a total of 640 cardiac cycle signals were analyzed in order to evaluate the relationship between the proposed auditory spectro-features and the severity of vascular access stenosis. As described in Sect. 2.1, the data were obtained from 16 hemodialysis patients with upper arm straight type AV grafts under different DOS conditions. Furthermore, the bruits were obtained at both the A-site and the V-site of each patient in order to evaluate the most suitable placement of the acoustic transducer for vascular access stenosis detection. In accordance with [26], the severity of the obstruction in the VA access was quantified using the DOS metric. The DOS is measured using angiography and defined as the area ratio of the luminal narrowing segment compared to that of the normal vascular segment, i.e.,

$$\mathrm{DOS} = \left(1 - \frac{d_r^2}{D_u^2}\right) \times 100\,\%, \tag{10}$$

where $d_r$ is the residual lumen diameter at the location of maximum stenosis and $D_u$ is the unobstructed lumen diameter, as shown in Fig. 3.

For the 16 participants, the DOS ranged from 8 to 98 % and had a mean value of 64 %. Generally speaking, a DOS of more than 50 % is considered to indicate vascular access stenosis. Moreover, based on clinical experience, a DOS of more than 70 % is taken to indicate a significant vascular access stenosis condition. Utilizing these definitions of the 32 sites considered in the present study (i.e., 16 A-sites and 16 V-sites), 18 sites indicated a significant access stenosis condition, while 14 sites indicated a non-significant access stenosis condition.

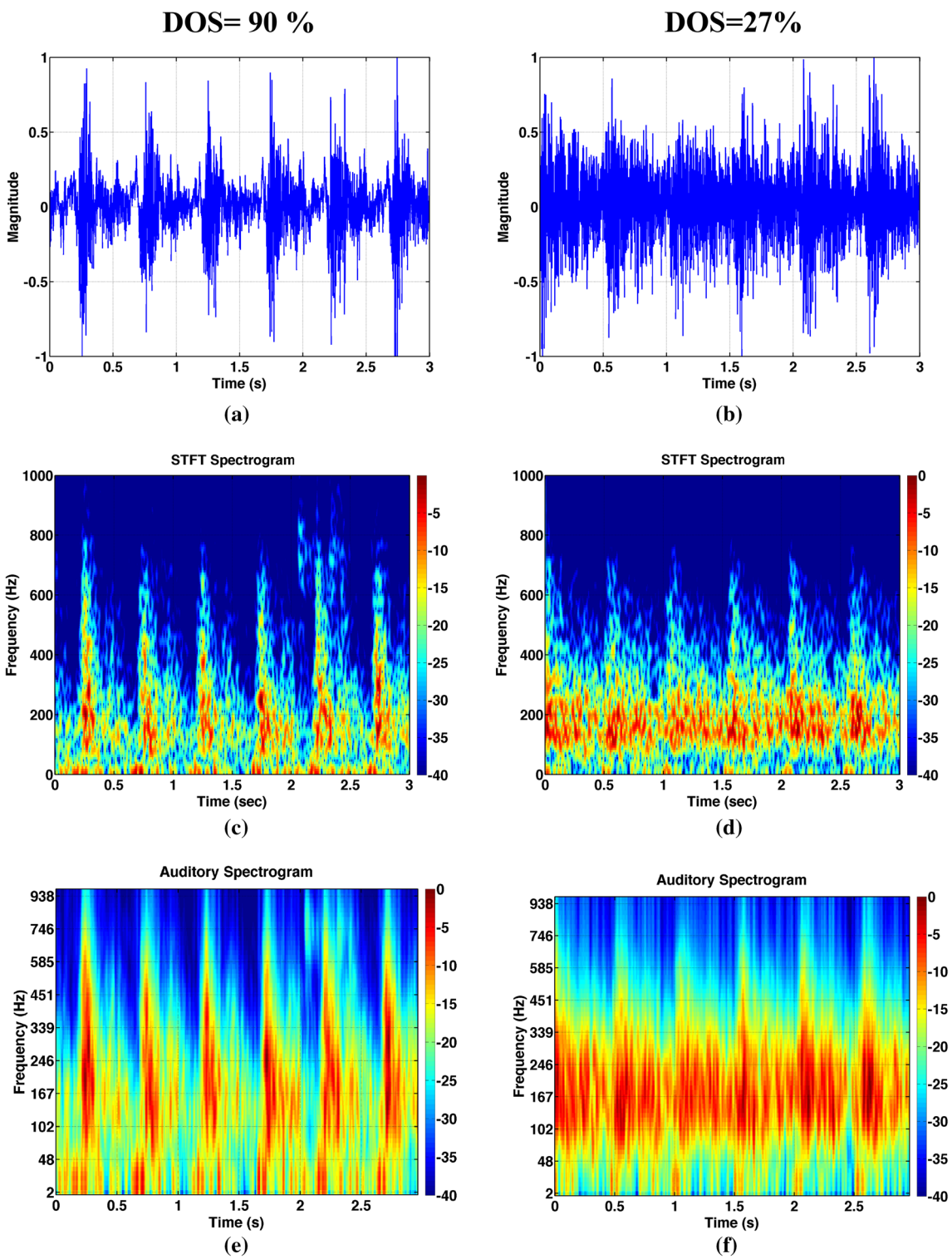


**Fig. 4** *Left side* **a** waveform, **c** STFT spectrogram and **e** auditory spectrogram of phonoangiography at the condition, DOS of 90 %, respectively. The *right side* is **b** waveform, **d** STFT spectrogram and **f** auditory spectrogram of phonoangiography at the condition, DOS of 27 %

Figure 4 shows the phonoangiography waveforms, STFT spectrograms and auditory spectrograms obtained for two cases with DOS values of 90 and 27 %, respectively. A qualitative difference in the phonoangiography waveforms recorded at A-sites of the two patients is clearly observed in Fig. 4a, b, respectively. Specifically, the systolic peaks in

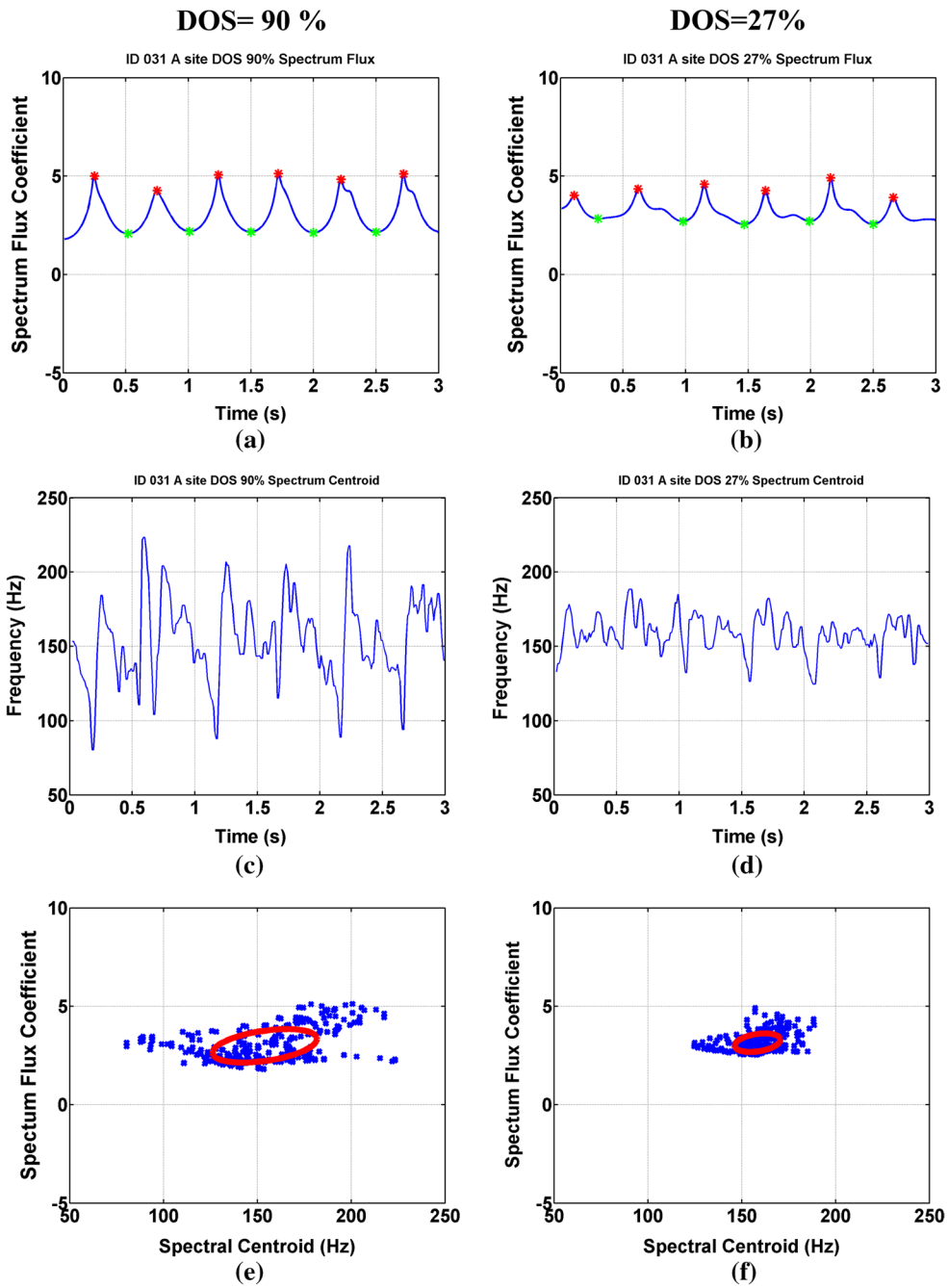


**Fig. 5** **a** Auditory spectrum flux, **c** auditory spectral centroid, **e** both 2D features at DOS of 90 % and **b** auditory spectrum flux, **d** auditory spectral centroid, **f** both 2D features at DOS of 27 %, respectively

the waveform corresponding to a significant DOS (Fig. 4a) are far sharper than those in the waveform corresponding to a normal DOS (Fig. 4b). Figure 4c, d shows the energy distributions of the two waveforms in the time–frequency plane, as calculated by STFT. Meanwhile, Fig. 4e, f shows the corresponding auditory spectrograms of the two waveforms. Note that in Fig. 4c–f, the *x*-, *y*- and *z*-axes represent time, frequency and magnitude, respectively. Comparing the four figures, it is noted that the auditory spectrograms provide a clearer visual representation of the energy distribution in the phonoangiography waveform than the STFT spectrograms. A detailed inspection of Fig. 4e shows that in the case of severe stenosis, the spectral energy is distributed over a broad range of 50–800 Hz and exist high-frequency components, which is induced by the turbulent flow through stenotic region at vascular access. However, for the case of normal stenosis, the energy is distributed over a more limited range of 50–450 Hz. Furthermore, the spectrogram has a flatter envelope profile for each cardiac cycle.

Although the auditory spectrograms provide a useful visualization of the phonoangiography waveform in the time–frequency domain, they are not amenable to

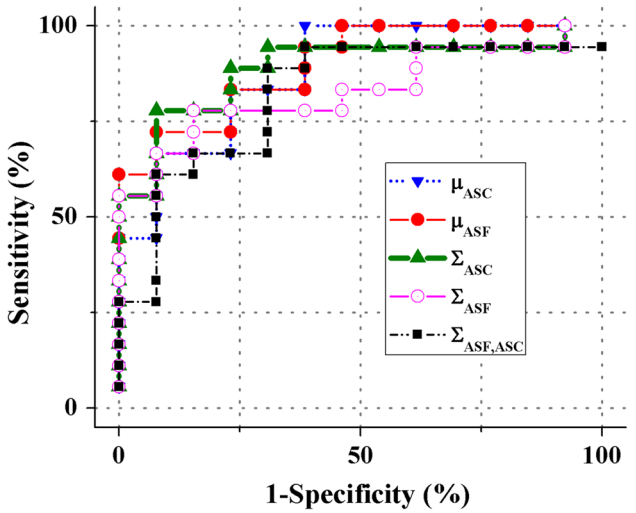


**Fig. 6** ROC curve of auditory spectro-temporal features extracted from bruits at A-site

**Table 1** Accuracy of the stenosis detector for different MGD feature sets

| Feature sets | AUC | Accuracy (%) | Sensitivity | Specificity |
|---|---|---|---|---|
| A-site | | | | |
| $\mu_{ASC}$ | 0.88 | 80.64 | 83.33 | 76.92 |
| $\mu_{ASF}$ | 0.90 | 80.64 | 83.33 | 76.92 |
| $\Sigma_{ASC}$ | 0.89 | 83.87 | 88.89 | 76.92 |
| $\Sigma_{ASF}$ | 0.83 | 80.65 | 88.89 | 69.23 |
| $\Sigma_{ASF,ASC}$ | 0.82 | 70.97 | 83.33 | 53.85 |
| V-site | | | | |
| $\mu_{ASC}$ | 0.51 | 64.52 | 66.67 | 61.54 |
| $\mu_{ASF}$ | 0.60 | 61.29 | 61.11 | 61.54 |
| $\Sigma_{ASC}$ | 0.81 | 70.97 | 77.78 | 61.54 |
| $\Sigma_{ASF}$ | 0.62 | 67.74 | 72.22 | 61.54 |
| $\Sigma_{ASF,ASC}$ | 0.70 | 70.97 | 88.89 | 46.15 |

$\mu_{ASC}$ is mean of auditory spectral centroid, $\mu_{ASF}$ is mean of auditor spectrum flux, $\Sigma_{ASC}$ is covariance matrix of auditory spectral centroid ($\Sigma_{11}$), $\Sigma_{ASF}$ is covariance matrix of auditory spectrum flux ($\Sigma_{22}$) and $\Sigma_{ASF,ASC}$ is covariance matrix between auditory spectral centroid and auditory spectrum flux ($\Sigma_{12}$ or $\Sigma_{21}$)

quantitative analysis. Thus, as described in Sect. 2.4, the auditory spectrograms of the bruits were quantified by means of their ASF and ASC features. Figure 5a, b shows the ASF values of the bruits corresponding to DOS values of 90 and 27 %, respectively. It is seen that both profiles have a similar regular periodic tendency due to the pulsatile nature of the local blood flow. However, the peaks in the flux envelope corresponding to DOS = 90 % are sharper than those in the envelope corresponding to DOS = 27 %. Figure 5c, d shows the ASC curves of the two bruits. It is seen that the ASC curve corresponding to DOS = 90 % exhibits a greater variation range than that corresponding to DOS = 27 %. Moreover, the peaks in the ASC curve (corresponding to high-pitch points) coincide with the cardiac cycle peaks in the case of severe stenosis (i.e., DOS = 90 %). Figure 5e, f shows the 2D features of the waveforms corresponding to DOS = 90 % and DOS = 27 %, respectively. The MGD function mentioned in Sect. 2.4 was used to describe the 2D features of both (as shown in the red solid lines in Fig. 5a, b). It is seen that in the case of severe stenosis, the elliptical circle of MGD is more widely distributed in the domain, whereas in the case of normal stenosis, the 2D features points are more densely packed.

In this study, the stenosis detection performance of the auditory spectro-temporal features was evaluated by means of the receiver operating characteristic (ROC) curve [15]. The ROC curve is widely used to visualize the achievable fraction between sensitivity and specificity for different decision thresholds of the MGD parameters, shown as Fig. 6. The results demonstrated that the MGD covariance matrix of ASC, $\Sigma_{ASC}$ is a good indicator for stenosis detection. The overall accuracy of each stenosis detector feature set was evaluated by measuring the area under the respective ROC curve (AUC), as listed in Table 1. Table 1 shows the AUCs of all feature sets at A-site is larger than 0.80. However, only the MGD covariance matrix of ASC achieves 0.81 at V-site. The confusion matrix which composes four outcomes, namely true positive (TP), true negative (TN), false positive (FP) and false negative (FN), was used to evaluate the accuracy. The TP group comprised the patients with significant vascular access stenosis; the TN group comprised the patients without significant stenosis. The FP group comprised the normal patients wrongly identified as having significant vascular access stenosis, while the FN group comprised the patients with significant vascular access stenosis but wrongly identified as having normal vascular access stenosis. Table 1 shows the accuracy, sensitivity and specificity of the various features considered in the present study. It is seen that the accuracy of all feature sets at A-site are higher than V-site. Among the features, the MGD covariance matrix of the ASC at A-site and V-site yield better accuracy of 83.87 and 70.97 %, respectively.

## 4 Discussion

Previous studies have shown that the acoustic characteristics of vascular sound can be used to evaluate occluded blood vessels [17]. Moreover, it has been shown that SBA was used to investigate obstructed arteries [1]. In general, bruits are produced as the blood flows turbulently through the constricted portion of the blood vessel. Since the

turbulent flow results in spectral resonance, the detection of VA stenosis can be performed using spectral analysis methods [30]. Spectral analysis methods typically involve the cycle segmentation and performing an FFT to calculate the PSD of the analyzed signal. In previous study [9], the authors proposed a parametric method based on the Burg AR algorithm to overcome spectral leakage and smooth the PSD curve. The results showed that the difference in the Burg AR frequency spectra with and without occluded VA, respectively, provided an indication of VA stenosis. However, the accuracy of the Burg AR spectral analysis method is also dependent on the AR order and the choice of analyzed signal segment.

Various envelope-based extraction methods have been proposed for assisting in the segmentation of signals, including the Hilbert envelope and the Shannon energy envelope [11]. However, their performance is seriously degraded in noisy environments.

In clinical diagnoses, physicians auscultate the acoustic emission sounds from the body based on their intensity, pitch and temporal periodicity. An experienced physician can often recognize a stenotic blood flow condition based solely on the acoustic characteristics of the bruits. However, the diagnosis is intuitively skill dependent and subjective. Thus, more objective methods are required to support robust vascular access stenosis detection. The bruit pattern is too complicated to describe using only one-dimensional features. Thus, in the present study, the proposed auditory spectrogram is used to visualize the energy magnitude of the bruit pattern in the time and frequency domains simultaneously. The bruit induced by the blood flow through the vascular access has a pulsatile characteristic, and thus the change in the flow rate dominates the variation of the bruit pattern over time. As a consequence, the variation rate of the spectral energy in the auditory spectrogram, defined as the ASF, can be used to characterize the flow pattern of the bruits. For example, given a severe stenosis condition, the envelope of the ASF contains sharp peaks, which coincide with the systolic peaks in the cardiac cycles, as shown in Fig. 5a. By contrast, given a mild vascular access stenosis condition, the envelope of the spectrum flux is flatter and is characterized by a series of ripples rather than peaks, as shown in Fig. 5b. Thus, even though the spectrum flux envelope does not provide a precise indication of the flow velocity (as in Doppler ultrasonography, for example), the shape tendency of the flux profile provides a good qualitative indication of the presence (or otherwise) of stenosis.

The variation of the bruit pitch is also an essential characteristic in determining the severity of VA access stenosis. In the present study, the bruit pitch is quantified using the ASC feature, as shown in Fig. 5c, d. In general, the results obtained in this study have shown that a severe stenosis condition results in a higher pitch variation than that produced under moderate (DOS = 27 %) stenosis conditions. However, neither the ASC feature nor the auditory spectral flux feature provides sufficient information to permit the automatic recognition of vascular access stenosis. Thus, in the present study, the two features have been combined into a single ASC–ASF domain. The distribution of the data points in the ASC–ASF domain can describe by MGD model or other data-clustering model (i.e., support vector machine or *k*-nearest neighbor algorithm) to classify the stenosis and non-stenosis condition. Based on this classification model, the proposed system can be integrated with automatic stenosis detection system to realize the clinical application.

In this study, the bruits were recorded at both the A-site and the V-site of each patient in order to evaluate which of the two positions provided more reliable feature information for stenosis detection. Table 1 shows that the auditory spectro-temporal features extracted from the A-site yield a better performance than those extracted from the V-site. However, previous studies [4, 19] have shown that stenosis most commonly occurs nearly the V-site. It was shown in a previous numerical study that the blood flow upstream of a stenotic region has the form of steady laminar flow, whereas that downstream of the stenotic region has the form of turbulent flow [38]. As a result, the bruit sound patterns downstream of the stenotic region are unstable. However, the characteristic of the blood flow through constricted blood vessel is complicated. The suitable recording position can be further studied by the combination use of the Doppler ultrasonography.

## 5 Conclusions

Current AV graft stenosis surveillance methods based on static dialysis venous pressure, flow monitoring and duplex ultrasound involve the use of sophisticated and expensive equipment, and are therefore impractical for use in the home. Accordingly, the present study has proposed an auditory auscultation method for detecting vascular access stenosis by means of a simple phonoangiography procedure. The performance of traditional stenosis detection methods based on a spectral analysis of the phonoangiography waveform is limited by the selection of the analyzed window and the frequency resolution. Moreover, the outcome of the detection process is significantly dependent on the skill and experience of the practitioner. Therefore, in the present study, a CWT module which mimics the hearing response of the human ear has been used to represent the phonoangiography signal in the form of an auditory spectrogram in the frequency-time domain. Furthermore, two spectro-temporal features, namely ASF and ASC, have been extracted from the auditory spectrogram and used to characterize the

relationship between the bruits and the DOS by means of a MGD model. Although the parameters of the MGD model are unable to provide an exact indication of the DOS, the results have shown that they have a sensitivity of 88.89 % and an accuracy of 83.87 % in predicting the occurrence of significant vascular access stenosis.

In summary, the results obtained in this study suggest that the proposed system provides a suitable basis for the development of a noninvasive stenosis surveillance method capable of use in the home by the hemodialysis patient or an untrained assistant. In future studies, additional auditory spectro-temporal features will be extracted and combined with an automatic recognition system in order to provide a more precise indication of the actual DOS condition.

**Acknowledgments** This study was supported by the National Cheng Kung University Hospital (protocol No. NCKUH-10305001) and in part of the National Science Council of the Republic of China under Grant No. NSC 100-2221-E-006-248-MY3. The institutional review board of National Cheng Kung University Hospital approved this study and the IRB No. ER-99-186. We are grateful to Sheng-Hsiang Lin and Jia-Ling Wu for providing the statistical consulting services from the Biostatistics Consulting Center, National Cheng Kung University Hospital.

## References

1. Akay YM, Welkowitz W, Semmlow JL, Kostis JB (1993) Noninvasive acoustical detection of coronary artery disease: a comparative study of signal processing methods. IEEE Trans Biomed Eng 40:571–578
2. Allon M, Robbin ML (2009) Hemodialysis vascular access monitoring: current concepts. Hemodial Int 13:153–162
3. Alvarez-Linera J, Benito-León J, Escribano J, Campollo J, Gesto R (2003) Prospective evaluation of carotid artery stenosis: elliptic centric contrast-enhanced MR angiography and spiral CT angiography compared with digital subtraction angiography. Am J Neuroradiol 24(5):1012–1019
4. Asif A, Gadalean FN, Merrill D, Cherla G, Cipleu CD, Epstein DL et al (2005) Inflow stenosis in arteriovenous fistulas and grafts: a multicenter, prospective study. Kidney Int 67:1986–1992
5. Athineos M, Ellis DPW (2007) Autoregressive modeling of temporal envelopes. IEEE Trans Signal Process 55:5237–5245
6. Avendaño-Valencia LD, Godino-Llorente JI, Blanco-Velasco M, Castellanos-Dominguez G (2010) Feature extraction from parametric time-frequency representations for heart murmur detection. Ann Biomed Eng 38:2716–2732
7. Bereksi-Reguig F, Debbal SM (2006) Cardiac murmur analysis using the short-time Fourier transform. J Mech Med Biol 6:273–284
8. Chen WL, Chen T, Lin CH, Chen PJ, Kan CD (2003) Phonographic signal with a fractional-order chaotic system: a novel and simple algorithm for analyzing residual arteriovenous access stenosis. Med Biol Eng Comput 51:1011–1019
9. Chen WL, Kan CD, Lin CH, Chen T (2014) A rule-based decision-making diagnosis system to evaluate arteriovenous shunt stenosis for hemodialysis treatment of patients using fuzzy petri nets. IEEE J Biomed Health Inform 18:703–713
10. Cherif LH, Debbal SM, Bereksi-Reguig F (2010) Choice of the wavelet analyzing in the phonocardiogram signal analysis using the discrete and the packet wavelet transform. Expert Syst Appl 37:913–918
11. Choi S, Jiang Z (2008) Comparison of envelope extraction algorithms for cardiac sound signal segmentation. Expert Syst Appl 34:1056–1069
12. Dhingra RK, Young EW, Hulbert-Shearon TE, Leavey SF, Port FK (2001) Type of vascular access and mortality in U.S. hemodialysis patients. Kidney Int 60:1443–1451
13. Diegeler A, Thiele H, Falk V, Hambrecht R, Spyrantis N, Sick P et al (2002) Comparison of stenting with minimally invasive bypass surgery for stenosis of the left anterior descending coronary artery. N Engl J Med 347:561–566
14. Ergen B, Tatar Y, Gulcur HO (2012) Time–frequency analysis of phonocardiogram signals using wavelet transform: a comparative study. Comput Methods Biomech Biomed Engin 15:371–381
15. Fawcett T (2006) An introduction to ROC analysis. Pattern Recogn Lett 27:861–874
16. Feldman HI, Kobrin S, Wasserstein A (1996) Hemodialysis vascular access morbidity. J Am Soc Nephrol 7:523–535
17. Fredberg JJ (1977) Origin and character of vascular murmurs: model studies. J Acoust Soc Am 61:1077–1085
18. Gianfelici F, Biagetti G, Crippa P, Turchetti C (2007) Multicomponent AM–FM representations: an asymptotically exact approach. IEEE Trans Audio Speech Lang Process 15:823–837
19. Glasberg BR, Moore BCJ (1990) Derivation of auditory filter shapes from notched-noise data. Hear Res 47:103–138
20. Irino T, Patterson RD (2006) A dynamic compressive gammachirp auditory filterbank. IEEE Trans Audio Speech Lang Process 14:2222–2232
21. Knox R, Breslau P, Strandness DE (1981) Quantitative carotid phonoangiography. Stroke 12(6):798–803
22. Lee CM, Zhang YT (2003) Reduction of motion artifacts from photoplethysmographic recordings using a wavelet denoising approach. In: Biomedical engineering IEEE EMBS Asian-Pacific conference on, Nara, Japan, pp 194–195
23. Lees R (1984) Phonoangiography: qualitative and quantitative. Ann Biomed Eng 12:55–62
24. Lees RS, Dewey CF (1970) Phonoangiography: a new noninvasive diagnostic method for studying arterial disease. Proc Natl Acad Sci 67:935–942
25. Mansy HA, Hoxie SJ, Patel NH, Sandler RH (2005) Computerised analysis of auscultatory sounds associated with vascular patency of hemodialysis access. Med Biol Eng Comput 43:56–62
26. Maya ID, Oser R, Saddekni S, Barker J, Allon M (2004) Vascular access stenosis: comparison of arteriovenous grafts and fistulas. Am J Kidney Dis 44:859–865
27. Middleton WD, Picus DD, Marx MV, Melson GL (1989) Color Doppler sonography of hemodialysis vascular access: comparison with angiography. Am J Roentgenol 152(3):633–639
28. Rosen RM, Parthasarathy SP, Turner AF, Blankenhorn DH, Roschke EJ (1977) Phonoangiography by autocorrelation. Circulation 55(4):626–633
29. Schwab SJ, Oliver MJ, Suhocki P, McCann R (2001) Hemodialysis arteriovenous access: detection of stenosis and response to treatment by vascular access blood flow. Kidney Int 59(1):358–362
30. Semmlow JL, Akay M, Welkowitz W (1990) Noninvasive detection of coronary artery disease using parametric spectral analysis methods. IEEE Eng Med Biol 9:33–36
31. Seo J, Mittal R (2012) A coupled flow-acoustic computational study of bruits from a modeled stenosed artery. Med Biol Eng Comput 50:1025–1035
32. Sung P-H, Thompson WR, Wang J-N, Wang J-F, Jang L-S (2015) Computer-assisted auscultation: patent ductus arteriosus detection based on auditory time–frequency analysis. J Med Biol Eng. doi:10.1007/s40846-015-0008-9

33. Teng Z, Wiesel A, Greco MS (2013) Multivariate generalized gaussian distribution: convexity and graphical models. IEEE Trans Signal Process 61:4141–4148
34. Tessitore N, Mansueto G, Bedogna V, Lipari G, Poli A, Gammaro L et al (2003) A prospective controlled trial on effect of percutaneous transluminal angioplasty on functioning arteriovenous fistulae survival. J Am Soc Nephrol 14(6):1623–1627
35. Thomas S, Ganapathy S, Hermansky H (2008) Recognition of reverberant speech using frequency domain linear prediction. IEEE Signal Process Lett 15:681–684
36. Tzanetakis G, Cook P (2002) Musical genre classification of audio signals. IEEE Trans Speech Audio Process 10:293–302
37. U.S. Renal Data System, USRDS (2013) Annual data report: atlas of chronic kidney disease and end-stage renal disease in the United States. NIH, Bethesda 2013
38. Varghese SS, Frankel SH, Fischer PF (2007) Direct numerical simulation of stenotic flows. Part 2. Pulsatile flow. J Fluid Mech 582:281–318
39. Watanabe H, Muramatsu S, Kikuchi H (2010) Interval calculation of EM algorithm for GMM parameter estimation. In: Proceedings IEEE ISCAS 2010, Paris, France, pp 2686–2689
40. Wiese P, Nonnast-Daniel B (2004) Colour Doppler ultrasound in dialysis access. Nephrol Dial Transplant 19:1956–1963